Mathematical Modeling of an Inductive Link for Optimizing Efficiency

Hussnain Ali, *Student Member IEEE*, Talha J Ahmad, Shoab A Khan
Department of Biomedical Engineering
Center for Advanced Research in Engineering
Islamabad, Pakistan
hussnain@ieee.org, talhajamal@live.com, shoab@carepvtltd.com

***Abstract*—Design of an optimized RF transcutaneous link through inductive coils is an arduous design process which involves complex mathematical modeling to search for optimized design parameters. This paper presents a generalized model which encompasses all possible voltage driven circuit realizations of an inductive link and presents a comparison on the bases of link efficiency and voltage gain. Mathematical expressions for the generalized voltage driven model as well as for the equivalent circuit topologies are derived. Moreover effect of different parameters such as resonating impedances on the final relationships is exhaustively analyzed.**

Optimization is a critical aspect in designing inductive links for medical implants since the link virtually acts as an air-core transformer with relatively low mutual coupling. Therefore, in order to maximize the gain and improve the link efficiency it is very necessary to design the link on optimized parameters. Aim of the analysis is to facilitate the designers in their design process as mathematical relationships for different models and their comparison has never been reported earlier in literature.

Keywords **— Inductive Link; Wireless Data and Power Transmission; Inductive Coils**

I. INTRODUCTION

Ubiquity of inductive links for wireless data and power transmission applications such as implantable biomedical devices like Cochlear Implants, Retinal Implants, ICDs etc.; RFIDs; Body Area Networks (BAN); wireless chargers and telemetric applications demand efficient inductive links in order to maximize link efficiencies at low coupling ranges. Design requirements of an inductive link require careful consideration of (i) bandwidth for supporting high data rates; (ii) efficiency for least power drop across the link and; (iii) coupling insensitivity [1]. In the design of RF data and power transmission links efficient power transfer is a major bottle neck, not efficient data transfer [3]. A trade-off between data rate and power transmission efficiency needs to be established when using a single coil for both data and power transfer since efficient power transfer is achieved using low frequency while higher data rates are better supported by high frequency. This is due to the fact that human body is penetrable to magnetic fields at lower frequencies [6] i.e. power transfer is more efficient with high-coils, a requirement that can conflict with data transfer if a high bandwidth data link is necessary [3]. Two ways to cope with the problem are by (i) using separate coils operating at different frequencies for data and power transfer when no compromise between efficiency and data bandwidth is required, approach used by [6,7] and (ii) optimizing design parameters for efficiency and high data rates as reported in [2], [3].

First step in the design and analysis of an inductive link requires simplified circuit representation of the inductive link. Like every two port network, inductive links may be driven by either a current or a voltage source. In this paper, we would only consider voltage driven circuits and derive voltage gain and efficiency expressions for all possible voltage driven topologies and make a comparison. Many voltage driven topologies have been reported in literature. A brief overview is stated here. Simplest most circuit representation is found in [2, 5] which takes into account primary and secondary coil inductances, their self resistances and secondary load impedance (resistance in simplest case) to compute relationship of link efficiency to the coupling coefficient 'k'. Hmida et al. [2], however, has further decomposed the secondary impedance into a resonating capacitor in parallel with the secondary coil to compute link efficiency and voltage gain. Reference [1] incorporates parallel resonance both at primary and secondary, whereas [3] employs series resonance at primary and parallel resonance at secondary. Advantage of this scheme is its close proximity to the final circuit (if a power amplifier such as Class E is used). Zeirhofer et al. [4] uses similar equivalent representation but incorporates feedback in the link and performs a comprehensive frequency analysis on the resulting circuit. Every topology has its own advantages and disadvantages in terms of voltage gain, efficiency, and form factor to name a few.

This paper is divided as follows. In Section II, mathematical expressions of the generalized voltage driven model are first derived. Then by the help of this generalized model, voltage gain and efficiency expressions for the six equivalent topologies are derived one by one. Strengths and weaknesses of each topology are given and their individual relationships are depicted mathematically as well as graphically.

II. MATHEMATICAL DERIVATIONS

A. Generalized Models

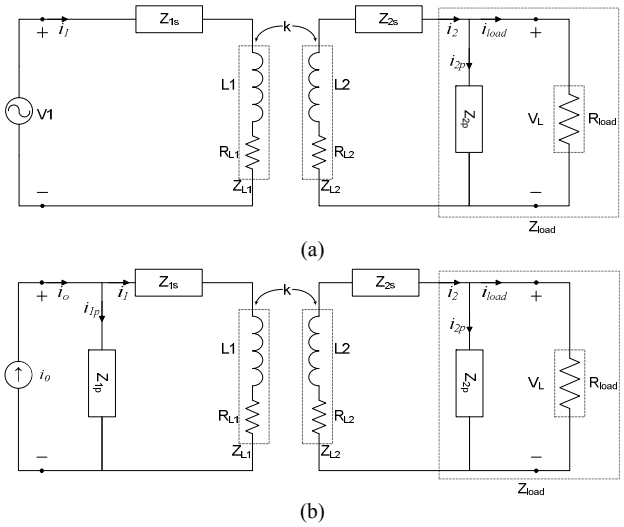

Figure 1: Generalized Circuit Models of inductive link (a) Voltage driven model; (b) current driven model.

The generalized voltage driven model and current driven model of the inductive link is depicted in Fig. 1a and Fig. 1b respectively. L_1 and L_2 represent inductive coils at primary and secondary side with their effective series resistances R_{L1} and R_{L2}. Z_{1s} and Z_{2s} are the series resonance impedances (capacitors) whereas Z_{1p} and Z_{2p} are parallel resonance impedances at primary and secondary side respectively.

Since we would analyze only voltage driven models in this paper, Fig. 1a would serve as our generalized voltage driven model. Equations (1)-(9) characterize this generalized voltage driven model. At one time either one of series or parallel resonance topologies should be employed which simplifies the model into six equivalent representations as given in Fig. 2 – Fig. 7.

$$i_2 = i_{2p} + i_L \tag{1}$$

$$Z_{ns} = 1/(j\omega C_{ns}) \tag{2}$$

$$Z_M = j\omega M = j\omega k\sqrt{L_1 L_2} \tag{3a}$$

$$Z_{Ln} = (j\omega L_n + R_{Ln}) \tag{3b}$$

$$Z_{load} = Z_{2p}||R_{load} \tag{3c}$$

$$(n = 1 \rightarrow primary; n = 2 \rightarrow secondary)$$

$$V_1 = (Z_{1s} + Z_{L1})i_1 - Z_M i_2 \tag{4}$$

$$V_L = -(Z_{2s} + Z_{L2})i_2 + Z_M i_1 \tag{5}$$

$$V_L = R_{load} i_L = Z_{load} i_2 \tag{6}$$

$$\frac{V_L}{V_1} = \frac{Z_M Z_{load}}{(Z_{1s} + Z_{L1})(Z_{2s} + Z_{L2} + Z_{load}) - Z_M^2} \tag{7}$$

$$i_1 = \frac{V_1 + Z_M(V_L/Z_{load})}{Z_{1s} + Z_{L1}} \tag{8}$$

$$\eta_{link} = \frac{Re[V_L I_L^*]}{Re[V_1 I_0^*]} = \frac{Re[V_L(V_L/R_{load})^*]}{Re[V_1].Re[I_0^*]} = \frac{|V_L|^2/R_{load}}{Re[V_1].Re[I_0^*]} \tag{9}$$

B. No Resonance Topology

Fig. 2a shows the equivalent model with no resonance at all. It acts like a simple transformer without any resonance impedances at either primary or secondary side. This model is not usually used in the actual designs but is given here as a reference to compare the link efficiency and voltage gain when resonance is applied.

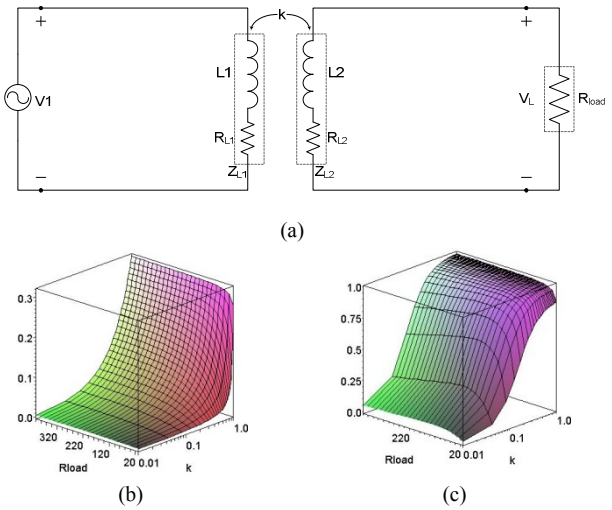

Figure 2: No resonance topology (a) Equivalent Model; (b) Voltage gain profile; (c) Link Efficiency profile of the equivalent topology

Voltage gain and link efficiency for this circuit is given by (10) and (11) respectively:

$$\frac{V_L}{V_1} = \frac{j\,\omega\,M\,R_{load}}{(\boldsymbol{A})\omega^2 + j\,(\boldsymbol{B})\omega + (\boldsymbol{D})} \tag{10}$$

$$\eta_{link} = \frac{R_{load}\,\omega^2 M^2}{\left((\boldsymbol{E})M^2 + R_{L1}{L_2}^2\right)\omega^2 + (R_{L1}(\boldsymbol{E})^2)} \tag{11}$$

where

$\boldsymbol{A} = M^2 - L_1 L_2$

$\boldsymbol{B} = \boldsymbol{C} + L_1 R_{load} = (L_1 R_{L2} + L_1 R_{load} + L_2\, R_{L1})$

$\boldsymbol{C} = L_1 R_{L2} + L_2\, R_{L1}$

$\boldsymbol{D} = R_{L1} R_{load} + R_{L1} R_{L2}$

$\boldsymbol{E} = R_{load} + R_{L2}$

It can be inferred from the above set of equations and graphs shown in Fig. 2 that voltage gain is highly dependent upon coupling coefficient, $k = M/\sqrt{L_1 L_2}$, as well as quality factor $Q_L = (\omega L)/R_L$, which implies that effective resistance of the coupled coils (R_L) must be as low as possible for maximum efficiency.

C. Series tuned Primary Circuit

Fig. 3a depicts an equivalent model with a series capacitor at primary side. This topology is a good example to analyze the effect of series resonance impedance on the link alone. Equations (7) and (8) are substituted with $C_{2p} = 0$ & $C_{2s} = \infty$. Resulting expressions for gain is given by:

$$V_L/V_1 = \frac{j\,C_{1s}\,\omega^2\,M\,R_{load}}{\big(C_{1s}(\boldsymbol{A})\big)\omega^3 + j\big(C_{1s}(\boldsymbol{B})\big)\omega^2 + (C_{1s}(\boldsymbol{D}) + L_2)\omega - j(\boldsymbol{E})} \tag{12}$$

Link efficiency is same as that given by (11) which implies series impedance at primary side has no effect on link efficiency. It can further be deduced that resonance impedances incorporated at primary side in the design only effect the voltage gain but not the link efficiency.

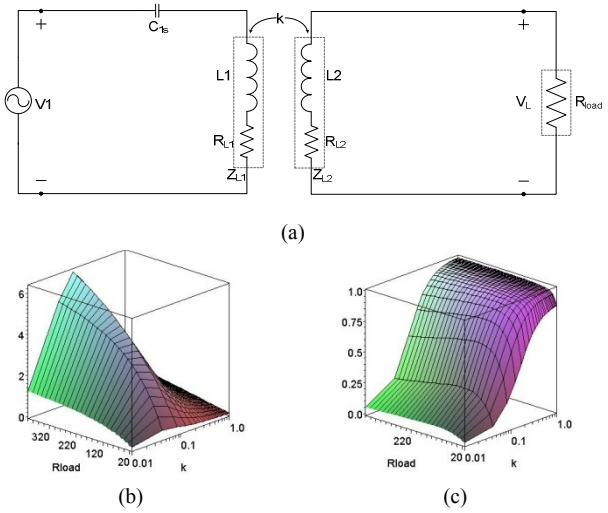

Figure 3: Series tuned primary circuit (a) Equivalent Model; (b) Voltage gain profile; (c) Link Efficiency profile of the equivalent topology

D. Series tuned Secondary Circuit

Fig. 4a depicts an equivalent model with a series capacitor at secondary side and no resonance at primary side. Equations (7) and (8) are substituted with $C_{2p} = 0$ & $C_{1s} = \infty$. Resulting expressions for voltage gain and efficiency are given by (13) and (14) respectively:

$$\frac{V_L}{V_1} = \frac{j\,M\,R_{load}C_{2s}\omega^2}{\big(C_{2s}(\boldsymbol{A})\big)\omega^3 + j\big(C_{2s}(\boldsymbol{B})\big)\omega^2 + (C_{2s}(\boldsymbol{D}) + L_1)\omega - j(R_{L1})} \tag{13}$$

$$\eta_{link} = \frac{R_{load}w^4{C_{2s}}^2M^2}{\Big({C_{2s}}^2(\boldsymbol{F})\Big)\omega^4 + (\boldsymbol{G})\omega^2 + (R_{L1})} \tag{14}$$

where

$\boldsymbol{F} = \Big({L_2}^2R_{L1} + M^2(\boldsymbol{E})\Big)$

$\boldsymbol{G} = \big({C_{2s}}^2R_{L1}(\boldsymbol{E})^2 - 2R_{L1}L_2C_{2s}\big)$

Voltage gain and efficiency profiles with respect to R_{load} and coupling coefficient k are shown in Fig. 4b and 4c respectively.

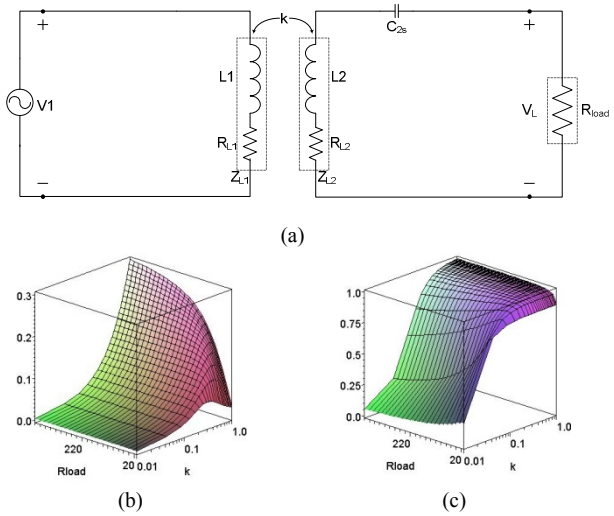

Figure 4: Series tuned secondary circuit (a) Equivalent Model; (b) Voltage gain profile; (c) Link Efficiency profile of the equivalent topology

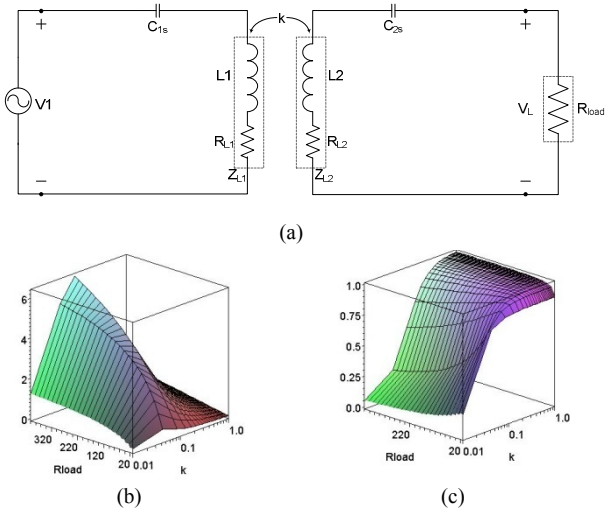

Figure 5: Series tuned primary and secondary circuit (a) Equivalent Model; (b) Voltage gain profile; (c) Link Efficiency profile of the equivalent topology

E. Series tuned Primary and Secondary Circuit

Combing the effects of two above topologies and resonating primary and secondary side with series capacitances, as shown in Fig. 5a, results in voltage again given by (15).

$$\frac{V_L}{V_1} = \frac{jM\,R_{load}C_{1s}C_{2s}\omega^3}{C_{1s}C_{2s}[(\boldsymbol{A})\omega^4 + (\boldsymbol{B})\omega^3 + (\boldsymbol{D}+\boldsymbol{H})\omega^2] - j(\boldsymbol{I})\omega - 1} \tag{15}$$

where $\boldsymbol{H}$ and $\boldsymbol{I}$ are given by:

$\boldsymbol{H} = L_1C_{1s} + L_2C_{2s}$

$\boldsymbol{I} = C_{2s}(\boldsymbol{E}) + R_{L1}C_{1s} = C_{2s}(R_{L2} + R_{load}) + R_{L1}C_{1s}$

Link efficiency for this topology is same that of series tuned secondary circuit i.e. (14) owing to the fact that primary resonance has no effect on link efficiency.

F. Parallel Tuned Secondary Side

Fig. 6a is a popular topology with a parallel resonating capacitor at the secondary side. Conditions applied to the generalized model are: $C_{1s} = C_{2s} = \infty$. Hmida et al. [2] has further exploited the design equations for efficiency and has concluded that the link efficiency as well as voltage gain module given by a secondary circuit tuned in parallel resonance is better than that given by a secondary circuit tuned in series resonance in the coupling zone experienced by practical medical implants (k<0.45). This can be verified by voltage gain and link efficiency expressions (16) and (17) as well as respective profiles depicted in Fig. 6b and Fig. 6c for this topology.

$$\frac{V_L}{V_1} = \frac{\omega\,M\,R_{load}}{R_{load}\,C_{2p}\big[(\boldsymbol{A})\omega^3 + j\big((\boldsymbol{C}) - (\boldsymbol{A})\big)\omega^2\big] + \big(R_{load}(\boldsymbol{J}) + (\boldsymbol{C})\big)\omega + j(\boldsymbol{D})} \tag{16}$$

$$\eta_{link} = \frac{\omega^2\,M^2\,R_{load}}{{R_{load}}^2\big[\big({C_{2p}}^2\,(\boldsymbol{K})\omega^4\big) + (R_{L1}(\boldsymbol{L}) + \boldsymbol{F})\omega^2\big] + (R_{L1}(\boldsymbol{E})^2)} \tag{17}$$

where

$\boldsymbol{J} = \big(L_1 + R_{L1}R_{L2}C_{2p}\big)$

$\boldsymbol{K} = (R_{L2}\,M^2 + {L_2}^2R_{L1})$

$\boldsymbol{L} = \big({C_{2p}}^2{R_{L2}}^2 - 2C_{2p}L_2\big)$

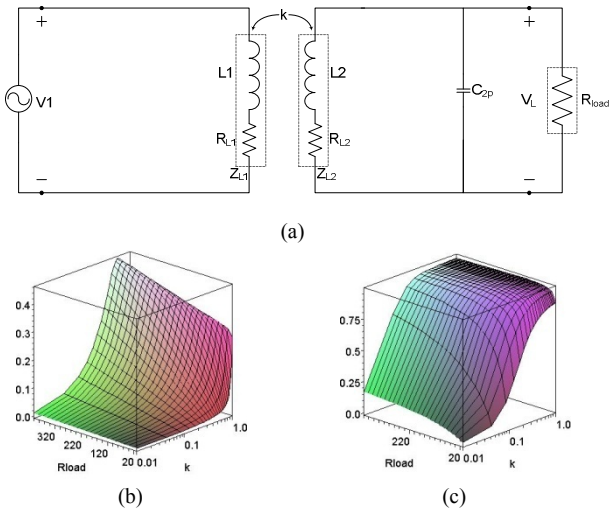

Figure 6: Parallel tuned secondary circuit (a) Equivalent Model; (b) Voltage gain profile; (c) Link Efficiency profile of the equivalent topology

G. *Series Tuned Primary and Parallel Tuned Secondary Circuit*

Finally, series tuned primary circuit and parallel tuned secondary circuit as shown in Fig. 7a is an ideal topology due to its high voltage gain and efficiency characteristics at low coupling ranges and its close resemblance with the actual link if a power amplifier is used at the primary side. Derived expressions for this topology can be expressed as:

$$\frac{V_L}{V_1} = \frac{C_{1s}\, R_{load}\, M\, \omega^2}{\left(C_{1s}R_{load}C_{2p}(\boldsymbol{A})\right)\omega^4 + j(\boldsymbol{M})\omega^3 + (\boldsymbol{N})\omega^2 + i\,(\boldsymbol{O})\omega + (\boldsymbol{E})} \tag{18}$$

where

$$\boldsymbol{M} = C_{1s}R_{load}C_{2p}(\boldsymbol{C}) - C_{1s}(\boldsymbol{A})$$

$$\boldsymbol{N} = C_{1s}(\boldsymbol{B}) + R_{load}C_{2p}(R_{L1}C_{1s}R_{L2} + L_2)$$

$$\boldsymbol{O} = R_{L1}C_{1s}(\boldsymbol{E}) + R_{L2}C_{2p}R_{load} + L_2$$

Link efficiency of this profile is given by (17); same that given by the parallel tuned secondary side, verifying the fact that adding series resonance at primary alters voltage gain only and there is no difference in link efficiency. Fig. 7b and 7c show voltage gain and link efficiency profiles for this topology.

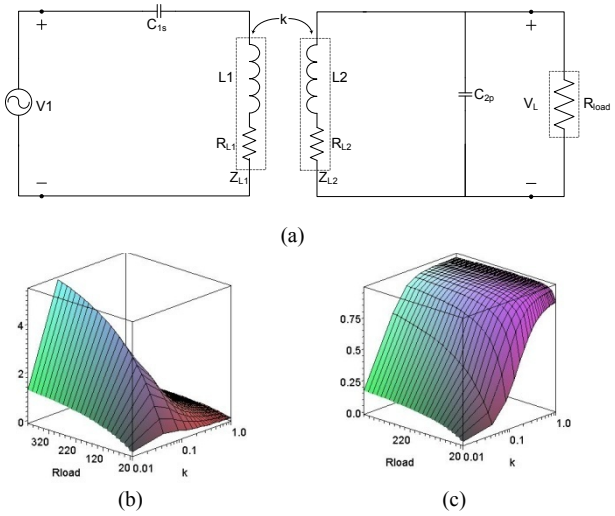

Figure 7: Series tuned primary and parallel tuned secondary circuit (a) Equivalent Model; (b) Voltage gain profile; (c) Link Efficiency profile of the equivalent topology

Another advantage of this scheme is that a series-resonant primary network requires lower input voltage swings due to nullification of the phase of the inductor and capacitor voltage at resonance [3].

III. Resonance Condition

Fig. 8 shows efficiency and voltage gain profiles of the circuit given in Fig. 7a with series impedance at the primary and parallel impedance at the secondary side. The profile elucidates the effect of resonating impedances added at primary and secondary side on voltage gain and link efficiency.

Resonance is achieved on the following condition:

$$j\omega L = {}^{1}/_{j\omega C}$$

We designed an inductive link on the parameters given in Table I. Operating frequency was set at $2.5MHz$ while $R_{load} = 127\Omega$. Maximum gain and efficiency peaks are clearly evident at resonance condition from the graphs shown in Fig. 8.

TABLE I.
Coil Parameters At Primary And Secondary Side

Primary	*Secondary*
L_1=80μH	L_2=8μH
R_{L1}=2.5Ω	R_{L2}=1.4Ω
C_{1s}=5.07x10^{-10}	C_{2p}=5.07x10^{-10}

IV. Conclusion

A generalized inductive link model to characterize all possible circuit realizations of a voltage driven inductive link has been reported. Generalized equations for this model as well as for different subsets of possible realizations has also been derived.

With reference to the above derived relationships and graphs depicted in Fig. 2 – Fig. 8, following major results and conclusions are made:

- Both Voltage Gain and Link Efficiency are highly dependent upon the coupling coefficient as well as Quality Factor of the coil.
- Resonating the secondary circuit by either series or parallel resonance remarkably improves the link efficiency and voltage gain.
- Resonance at primary side alters voltage gain only whereas resonance at secondary side alters both voltage gain and efficiency.

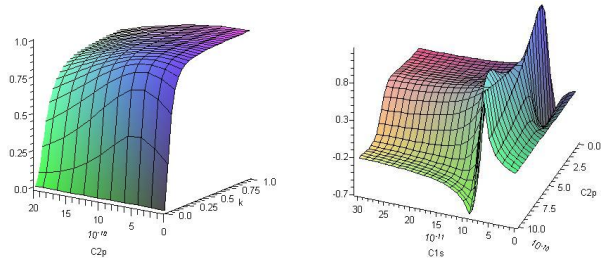

Figure 8: (a) Efficiency and (b) Voltage gain profile of series tuned primary and parallel tuned secondary side elucidating the resonance condition.

- Series Resonating Capacitor at primary side alters the Voltage Gain Profile however shunt resonating capacitor has no effect on either the voltage gain or the Link Efficiency.

These results imply that series resonating impedance at the primary side causes voltage across the primary coil to increase and therefore voltage developed at secondary side is increased proportionally. However, the ratio of voltage increase remains constant, i.e. link efficiency is unaltered.

- Incorporating resonance impedances into the design results in more and more dependence upon the frequency.

This result implies that resonance circuits make the final circuit band limited. Beside the advantage of better link efficiency and voltage gain, a requirement for efficient power transmission, they may not be suitable for wideband applications, which impose a serious constraint on data transfer.

REFERENCES

[1] Songping Mai, Chun Zhang, Mian Dong, Zhihua Wang, "A Cochlear System with Implant DSP", Proceedings: International Conference on Acoustics, Speech and Signal Processing (ICASSP), IEEE, vol. 5, pp. V-125-V-128, May 2006.

[2] Ghazi Ben Hmida, Hamadi Ghairani and Mounir Samet, "Design of a Wireless power and Data Transmission Circuits for Implantable Biomicrosystem", Biotechnology, Vol 6, pp. 153-164, 2007.

[3] Michael W. Baker, Rahul Sarpeshkar, "Feedback Analysis and Design of RF Power Links for Low-Power Bionic Systems", IEEE Transactions on Biomedical Circuits and Systems, vol. 1, pp: 28-38, March 2007.

[4] Clemens M. Zierhofer, Erwin S. Hochmair, "High-efficiency coupling-insensitive transcutaneous power and data transmission via an inductive link", IEEE Transactions on Biomedical Engineering, vol. 37, pp. 716-722, July 1990.

[5] Michael Catrysse, Bart Hermans, Robert Puers, "An Inductive Power System with integrated bi-directional Data-transmission", Proceedings: The 17th European Conference on Solid-State Transducers, vol. 115, pp. 221-229, September 2004.

[6] Bharatram Satyanarayanan Pundi, "Class-E Power Amplifier Design and Back-Telemetry Communication for Retinal Prosthesis", MS Thesis, North Carolina State University, Raleigh, North Carolina, 2002.

[7] Suresh Atluri, "A Wideband Power Efficient Inductive link for Implantable Biomedical Devices using Multiple Carrier Frequencies", MS Thesis, North Carolina State University, Raleigh, North Carolina, 2006.

[8] Galbraith, Douglas C.; Soma, Mani; White, Robert L., "A Wide-Band Efficient Inductive Transdennal Power and Data Link with Coupling Insensitive Gain,"*Biomedical Engineering, IEEE Transactions on* , vol.BME-34, no.4, pp.265-275, April 1987.